

Thalamic stimulation induced changes in effective connectivity

Nicholas M. Gregg¹, Gabriela Ojeda Valencia², Harvey Huang², Brian N. Lundstrom¹, Jamie J. Van Gompel³, Kai J. Miller³, Gregory A. Worrell^{1*}, Dora Hermes^{2*}

Affiliations:

1. Department of Neurology, Mayo Clinic, Rochester, MN
2. Department of Physiology and Biomedical Engineering, Mayo Clinic, Rochester MN
3. Department of Neurosurgery, Mayo Clinic, Rochester MN

* contributed equally

Correspondence:

Nicholas Gregg, MD: gregg.nicholas@mayo.edu

Dora Hermes, PhD: hermes.dora@mayo.edu

Gregory Worrell, MD PhD: worrell.gregory@mayo.edu

Key words: deep brain stimulation, neuromodulation, iEEG, connectivity, electrophysiology, epilepsy

Abstract

Deep brain stimulation (DBS) is a viable treatment for a variety of neurological conditions, however, the mechanisms through which DBS modulates large-scale brain networks are unresolved. Clinical effects of DBS are observed over multiple timescales. In some conditions, such as Parkinson's disease and essential tremor, clinical improvement is observed within seconds. In many other conditions, such as epilepsy, central pain, dystonia, neuropsychiatric conditions or Tourette syndrome, the DBS related effects are believed to require neuroplasticity or reorganization and often take hours to months to observe. To optimize DBS parameters, it is therefore essential to develop electrophysiological biomarkers that characterize whether DBS settings are successfully engaging and modulating the network involved in the disease of interest. In this study, 10 individuals with drug resistant epilepsy undergoing intracranial stereotactic EEG including a thalamus electrode underwent a trial of repetitive thalamic stimulation. We evaluated thalamocortical effective connectivity using single pulse electrical stimulation, both at baseline and following a 145 Hz stimulation treatment trial. We found that when high frequency stimulation was delivered for >1.5 hours, the evoked potentials measured from remote regions were significantly reduced in amplitude and the degree of modulation was proportional to the strength of baseline connectivity. When stimulation was delivered for shorter time periods, results were more variable. These findings suggest that changes in effective connectivity in the network targeted with DBS accumulate over hours of DBS. Stimulation evoked potentials provide an electrophysiological biomarker that allows for efficient data-driven characterization of neuromodulation effects, which could enable new objective approaches for individualized DBS optimization.

Introduction

Deep brain stimulation (DBS) is a viable treatment option for a variety of medication refractory neurological disorders. The efficacy of DBS was first demonstrated in 1987 in a patient with Parkinson's disease¹. The proportion of individuals that respond to DBS, and the degree of symptoms improvement differs between disorders, with particularly good results seen in disorders with well-defined pathological circuits and when DBS effects on clinical symptoms are immediate and allow for rapid screening and optimization of parameters (e.g. essential tremor, Parkinson's disease)².

DBS has demonstrated utility for other diseases, including drug resistant epilepsy³, however, the response rates and degree of symptom control may be less favorable in comparison to tremor disorders. In many cases, such as epilepsy, central pain and psychiatric conditions, DBS related effects are hypothesized to require neuroplasticity or reorganization and clinical effects take hours to months to observe⁴. Epilepsy is a disorder chiefly characterized by a predisposition to recurrent unprovoked epileptic seizures and associated comorbidities⁵. Substantial evidence has demonstrated that epilepsy is a brain network disorder, and notable for cross-subject heterogeneity, with subject-specific seizure network (SN) structure⁶, and non-stationary seizure risk profiles with daily and multiday cycles of risk⁷. The prototypical clinical manifestation of epilepsy—epileptic seizures—occur sporadically with inter-seizure intervals ranging from minutes to months. In such cases, it is essential to have rapid physiological biomarkers to quantify network level changes in excitability to inform seizure risk and guide therapy.

The setting of stereotactic EEG (sEEG), in which a number of multi-contact electrodes are used to characterize pathological networks and identify eloquent structures is highly suitable for developing such biomarkers. During sEEG, single pulse electrical stimulation can be used to evoke characteristic responses in connected regions, mapping effective connectivity throughout the network^{8,9}. This effective connectivity maps the causal influence of a stimulated site on other brain regions, and single pulse stimulation evoked potentials can quantify the excitability in such networks¹⁰⁻¹². Here, we test whether stimulation evoked potentials, as physiological biomarkers of effective connectivity, quantify meaningful neural changes after high frequency (HF) stim.

Results

Ten subjects with medication refractory epilepsy underwent clinically indicated invasive sEEG monitoring that included a thalamus electrode lead, and completed a trial of high frequency (HF) repetitive thalamic stimulation. Patient characteristics, sEEG lead location, and treatment stimulation parameters are listed in Table 1. Single pulses of electrical stimulation were delivered to the thalamus at baseline and following HF stimulation to quantify modulation of thalamocortical effective connectivity (thalamocortical evoked potentials) thought to be indicative of changes in network excitability¹⁰. Patient 1 completed bilateral anterior thalamus high frequency trial stimulation. Patient 6 underwent single pulse stimulation at baseline, after 1 hour of HF stimulation, and again after 5.75 hours of HF stimulation (listed HF stimulation durations reflect only the active phase of duty-cycle stimulation).

Patient	Age range (years)	Sex	Seizure onset	Thalamic stim. localization	All 145 Hz, duty cycle stim.	Duration thalamic HF stimulation	Med. change
1	16-20	m	Diffuse bifrontal, left hemisphere lead in	R-AM/AV/VAPc; L-AM/AV/VAPc	145 Hz, 90usec, 5.7mA (divided) 1m. on 1m. off	7 Hr	NC
2	46-50	m	Left middle temporal gyrus	L-AV/VLpd	145 Hz, 90 us, 3.6mA, continuous	1.2 Hr	NC
3	21-25	m	Bilateral hippocampus, left lead in	AM/AV, R-MTT, VAMc, VLpv, CeM	145 Hz, 200 us, 3.7mA, 1m. on 1m. off	1.8 Hr	NC
4	11-15	m	Right occipital, peri-lesion (perinatal stroke)	R-PuIM	145 Hz, 200 us, 5.8mA, 1m. on 3m. off	4.25 Hr	change (increase LTG, add ZNS 100 QHS)
5	16-20	f	Left hippocampus, peri-lesion (neoplasm)	L-VLpv	145 Hz, 200 us, 4.6mA, 1m. on 3 off	4.25 Hr	NC
6	66-70	f	Left neocortical and mesial temporal	L-VAPc/MTT	145 Hz, 200 us, 4.3mA, 1m. on 3 off	1; 5.75 Hr	NC
7	41-45	m	Bilateral anterior cingulate	R-VAPc	145 Hz, 200 us, 2.5mA, 1m. on 3 off	0.5 Hr	NC
8	16-20	f	Right superior temporal gyrus	R-VAPc	145 Hz, 200 us, 3.3mA, 1m. on 3 off	9.75 Hr	NC
9	6-10	f	Pre- and post-central gyri, peri-lesion (FCD)	L-VLpv	145 Hz, 200 us, 2.8mA, 1m. on 5 off	0.5 Hr	NC
10	16-20	f	Multifocal, right anterior/middle insula, amygdala, temporal neocortex	R-AV	145 Hz, 90 us, 3.2mA, 1m. on 5 off	0.75 Hr	Rescue IV lorazepam & LEV pre baseline

Table 1. Patient characteristics. The duration of thalamic high frequency stimulation is the active stimulation time (does not include off-phase of duty-cycle stimulation). L=left. R=right. FCD=focal cortical dysplasia. ANT=anterior nucleus of the thalamus. Thalamic nuclei abbreviations, Krauth/Morel atlas¹³. PuIM=medial pulvinar. AM=anteromedial nucleus. AV=anteroventral nucleus. VAPc=ventral anterior nucleus, parvocellular division. VLa=ventral lateral anterior nucleus. VLpv=ventral lateral posterior nucleus, ventral division. CeM=central medial nucleus. Duty-cycle (on-period and off-period) noted in minutes. NC=no change in regimen during the HF stimulation and single pulse stimulation period. LEV=levetiracetam.

Figure 1 provides a study overview. Thalamocortical effective connectivity was assessed in 10 patients, with a total of 11 thalamus leads. Thalamus electrodes targeted the anterior thalamus (n=9 subjects) with active contacts primarily positioned with the anterior complex (namely, anteromedial (AM) and anteroventral (AV) nuclei) or ventral group (ventral anterior (VA) and ventrolateral (VL) nuclei), and targeted the pulvinar (n=1 subject) with active contacts positioned in the medial pulvinar (PuIM). Evoked potential root mean square (RMS) amplitude was measured over the interval 20-300 milliseconds post single pulse stimulus for each recording contact, with example baseline and post-HF stimulation RMS amplitude shown in Fig. 2D. The time window of interest was selected to encompass typical N1 and N2 responses while omitting potential stimulation artifact⁸.

Figure 2 shows the 11 thalamus electrodes in MNI template space, overlaid on the Krauth/Morel thalamus atlas¹³, using the open-source Lead-DBS imaging package (v2.5.3)¹⁴, and BigBrain 3D human brain model¹⁵. Representative baseline and post-HF stimulation evoked

potentials are shown for two subjects, and group level modulation of thalamocortical effective connectivity (measured by effect size of modulation of RMS amplitude, Cohen-D).

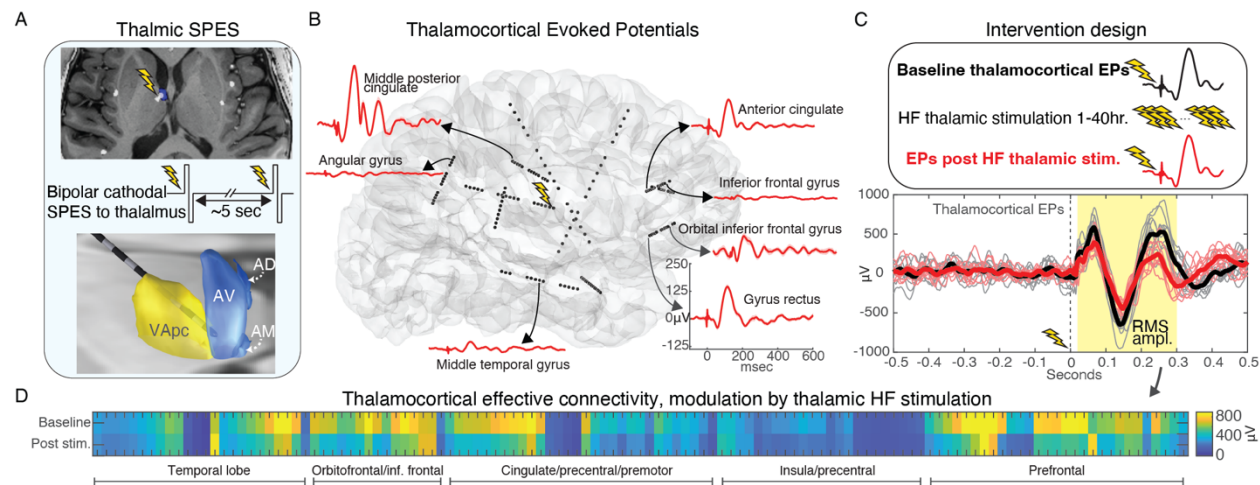


Figure 1. Thalamic high frequency stimulation and network effective connectivity. A) Bipolar single pulses of electrical stimulation (charge balanced symmetric square wave, leading cathodal phase) are delivered to neighboring thalamic electrode contacts. B) Single pulses delivered to the thalamus produce characteristic evoked responses in connected brain regions, evident in sEEG electrode voltage traces (figure shows representative evoked responses; average trace from $n=10$ single pulse stimuli). C) Thalamocortical evoked potentials were measured at baseline and following high frequency thalamic stimulation. Single trial and average voltage traces are shown for baseline (black) and post-high frequency stimulation (red). Root mean square (RMS) amplitude was calculated over post stimulus window 0.02-to-0.30 seconds, for each recording contact. D) Thalamocortical effective connectivity matrix shows evoked potential RMS amplitude at baseline, and post-high frequency stimulation, across all contacts, with clear suppression of thalamocortical evoked response amplitude (excitability) over multiple regions. AD=anterodorsal nucleus. AV=anteroventral nucleus. AM=anteromedial nucleus. VApc=ventral anterior nucleus, parvocellular division. SPES=single pulse electrical stimulation. EP=evoked potential. HF=high frequency.

Figure 2C shows a clear separation in induced changes in evoked potential amplitude with HF stimulation duration greater than or less than 1.5 hours. Consistent suppression of network excitability was seen with stimulation duration above 1.5 hours, which is not evident with short stimulation durations. Additionally, the degree of modulation is dependent on baseline effective connectivity, with positive correlation between baseline connectivity and modulation effect size. Fig. 2C only shows contacts with significant evoked potentials at baseline and ipsilateral to thalamic HF stimulation.

The anatomic distribution of HF stimulation induced changes are shown in glass brain renderings (Fig. 3). The anatomic distribution of effects are distinct across subjects, with different patterns seen with anterior complex (ex. Pt. 3), ventral group (ex. Pt 9), and pulvinar (Pt. 4) stimulation, with greater limbic, motor, and posterior quadrant patterns of connectivity, respectively. As evident in Figure 2C, Figure 3 again shows HF-stimulation induced changes in effective connectivity are dependent on stimulation duration.

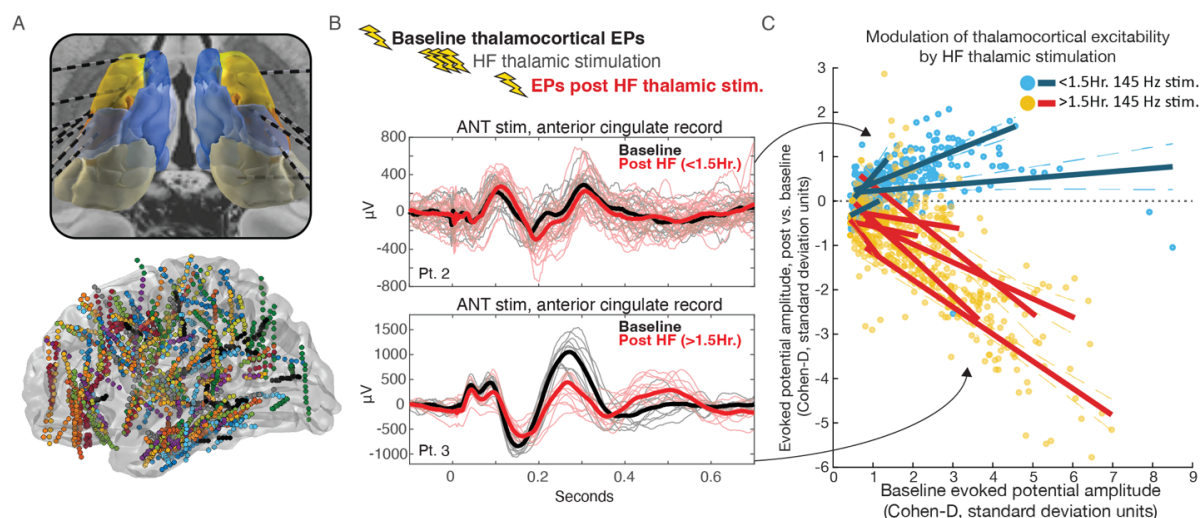


Figure 2. Thalamic high frequency stimulation modulates network effective connectivity and is dependent on baseline connectivity strength, and duration. A) Ten patient cohort with thalamus electrodes (top panel, Krauth/Morel thalamus atlas¹³) and all recording electrodes (bottom panel) shown in MNI template space (right hemisphere electrodes mirrored into left hemisphere). B) Example single trial and average thalamocortical evoked potential traces from two subjects completing short duration (top panel) and long duration (bottom panel) high frequency stimulation. C) Modulation of evoked potential amplitude is dependent on high frequency stimulation duration(>/< 1.5 hours of active high frequency stimulation), and the strength of baseline connectivity. Solid lines correspond to linear model fit for each individual (Patient 1 had bilateral thalamic stimulation and left and right hemispheres treated independently). Plot shows recording electrodes with statistically significant baseline evoked potentials (paired T-test comparing RMS amplitude 0.02:0.30 seconds post-single pulse stimulus to -0.48:-0.2 seconds pre-single pulse stim (voltage traces undergo baseline correction by subtracting the median value for window -0.2:-0.05 seconds pre stimulus)).

Discussion

Deep brain stimulation is an effective treatment for a number of neurological conditions, however, there is a limited understanding of the anatomical distribution, timescales, and mechanisms underlying DBS effects. Electrophysiological biomarkers of network engagement and network excitability are particularly needed for disorders—like epilepsy, central pain, neuropsychiatric conditions—without short latency clinical effects to assess and tune DBS.

Here, a unique cohort of individuals undergoing epilepsy sEEG monitoring that includes a thalamus electrode, demonstrates that thalamocortical effective connectivity (assessed by single pulse electrical stimulation) can identify network excitability changes induced by high frequency thalamic stimulation. This work demonstrates that high frequency thalamic stimulation induced changes are dependent on the duration of stimulation, with consistent suppression of network excitability occurring after >1.5 hours of active phase stimulation. Additionally, this approach maps the anatomical distribution of effects, which is critical important when assessing engagement of a pathological network. Multiple studies spanning neurological disorders amenable to DBS have shown that efficacy is dependent on pathological network engagement¹⁶⁻¹⁹ using imaging connectivity based measures of engagement. Effective

connectivity, which represents the direct causal influence between neural elements, may provide even greater insight into network engagement by thalamic subfield stimulation, when compared to structural or functional imaging based methods. These findings provide direct electrophysiological evidence to support the proposed “network hypothesis” for epilepsy deep brain stimulation efficacy seen in long-term follow up of the pivotal clinical trial of anterior nucleus of the thalamus DBS for epilepsy clinical.²⁰

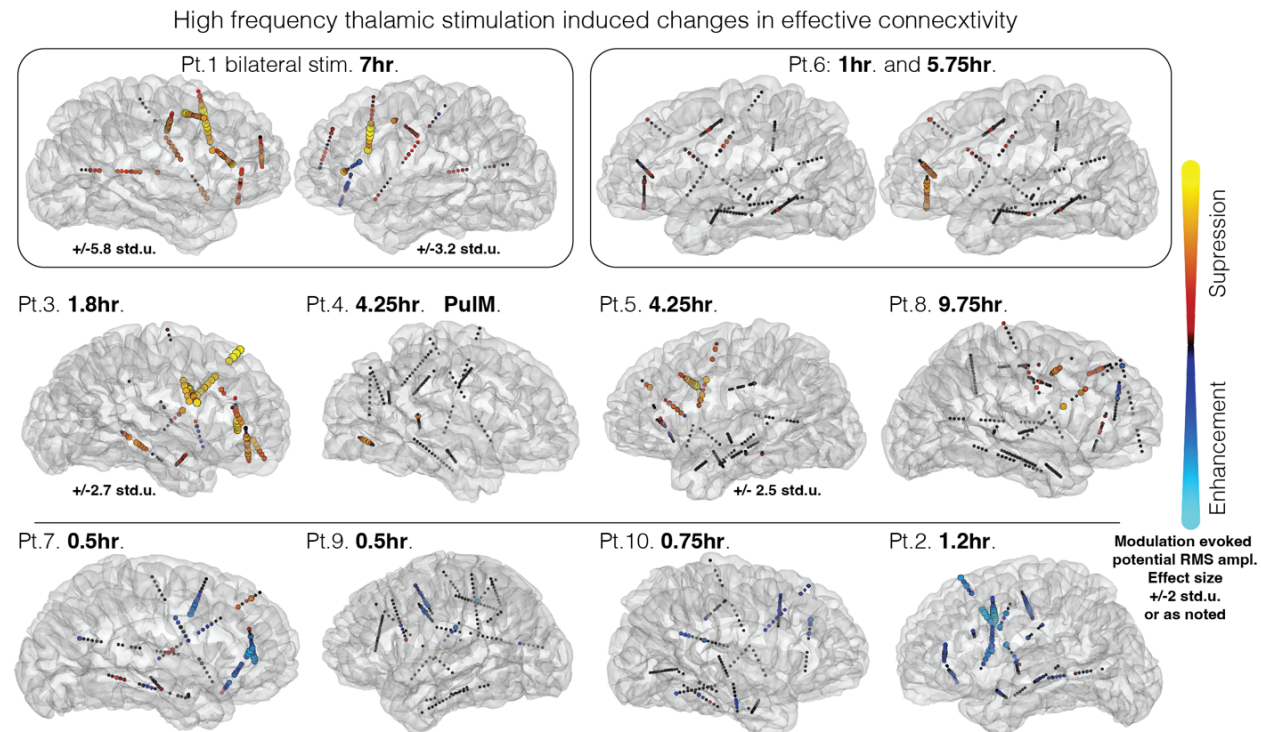


Figure 3. High frequency thalamic stimulation modulates brain excitability, with network specificity and stimulation duration dependence. Brain renderings show HF-stimulation induced changes in network effective connectivity (comparison of baseline and post-HF stimulation evoked potential RMS amplitude, Cohen-D effect size, for contacts with statistically significant baseline evoked potentials). Distinct anatomic distributions of effects can be seen between patients—note occipital engagement with medial pulvinar stimulation (Pt. 4), peri-rolandic engagement with ventrolateral nucleus stimulation (Pt. 4), and limbic engagement with anterior complex stimulation (ex. Pt. 3). Consistent suppression of effective connectivity is seen with HF stimulation duration >1.5 hours (top and middle row) vs. <1.5 hours (bottom row) (listed HF stimulation duration is the total time of the active phase only of duty-cycle stimulation). Std.u.=standard deviation units.

The 1.5 hours of active high frequency stimulation (does not include duty-cycle off phase) dependence may indicate that high frequency stimulation induced changes in thalamocortical effective connectivity reflect changes in neuronal activity regulated through homeostatic plasticity.²¹ Homeostatic plasticity operates to maintain relative stability in neuronal firing rates in the face of perturbations, and here may inhibit neuronal excitability in the face of HF stimulation. These hours long timescales observed here are also consistent with DBS clinical effects seen in motor tics, central pain, and mood symptoms⁴. Neuronal plasticity

dependent changes are distinct from the immediate direct electrical effects of DBS, which are evident in immediate tremor improvement in DBS for essential tremor and Parkinson's disease.

This work is limited by the relative rarity of human intracranial EEG that includes thalamus electrodes, and the unpredictability of clinical care. The high frequency thalamic stimulation was delivered as a part of clinical care using a pragmatic approach, contributing to differences in stimulation parameters. One patient had resumption of antiseizure medications after baseline single pulse stimulation measurements but before post-HF stimulation measurements, which might contribute to differences in network excitability. While the anterior nucleus of the thalamus was targeted in 9 subjects, there was variability in the exact thalamic subfield position of active contacts.

These findings suggest that changes in effective connectivity in the network targeted with DBS accumulate over hours of DBS. Stimulation evoked potentials provide an electrophysiological biomarker that allows for efficient data-driven characterization of neuromodulation effects, which could enable new objective approaches for individualized DBS optimization²².

Objective short-latency electrophysiology-based biomarkers of stimulation induced changes in brain excitability and network engagement may provide a new means of assessing stimulation targets and tuning stimulation parameters to ultimately improve neuromodulation. This work may be leveraged by emerging devices with chronic brain recordings and adaptive stimulation capabilities to enable a new paradigm of highly personalized neuromodulation.

Methods

This is a retrospective clinical case series evaluating the effects of clinical high frequency thalamic stimulation delivered during sEEG monitoring. All participants received research single pulse electrical stimulation to measure network effective connectivity. Following completion of seizure network characterization by invasive sEEG monitoring, patients may undergo a trial of clinical therapeutic stimulation to assess therapeutic benefit and side effects, with the advantage of high quality local field potential recordings from distributed brain regions (up to 256 recording contacts). Participants underwent research single pulse electrical stimulation delivered to thalamic sEEG electrode contacts during wakefulness to assess thalamocortical effective connectivity, with single pulse stimulation delivered preceding and following (within 1 hour) HF thalamic stimulation. The Institutional Review Board of Mayo Clinic gave ethical approval for this work. All patients in the study completed a written informed consent. Data will be made available upon reasonable request.

Patient characteristics are listed in Table 1. Single pulse bipolar stimulation was delivered in a bipolar fashion through immediately neighboring contacts on the same lead, using symmetric charge balanced biphasic stimulation pulses with leading cathodal phase, delivered at 0.2 Hz, with 200 microsecond pulse width, for 10-15 repetitions. Single pulse stimulation was delivered by a Natus Nicolet stimulator (Patients 1, 2, 7, 9), g.tec g.ESTIM PRO with g.HiAmp amplifier (Patients 4, 8), or Medtronic external neurostimulator 37022 (Patients 3, 5, 6, 10). Current clamped systems (Natus and g.tec) delivered single pulse stimuli at 6 mA, and voltage clamped (Medtronic) at 6 V. The Medtronic external neurostimulator was used to deliver HF thalamic stimulation for all subjects.

Thalamocortical evoked potential data were first cleaned of stimuli with excessive artifact. High pass (1 Hz), low pass (170 Hz) and bandstop (for 60 Hz line noise and harmonics (120 Hz and 180 Hz)) filtering was performed with fourth order Butterworth filters, with forward-reverse filtering to correct for phase distortion. Voltage trace baseline correction consisted of subtracting the median value for window -0.2 to -0.05 seconds pre-stimulus from the tracing. Lastly, adjusted common average referencing was performed as previously described²³.

To quantify the strength of effective connectivity, baseline evoked potential root mean square (RMS) amplitude was calculated over time window 20 milliseconds through 300 milliseconds post single pulse stimulus. The statistical significance of evoked potentials was assessed by paired t-test, comparing RMS amplitude over this window to a pre-stimulation period of equal duration (480 to 200 milliseconds pre-stimulus, which avoids the baseline correction window). Changes in network excitability are though to modulate the amplitude of stimulation evoked measures of effective connectivity. Here, modulation of excitability by HF stimulation was evaluated using Cohen's *d*, as has been used previously¹⁰, with Cohen's *d* effect size equal to the difference in mean evoked potential RMS amplitude (post-HF stimulation vs. baseline) divided by the pooled standard deviation. A linear regression model, using Ordinary Least Squares evaluated the association between baseline effective connectivity, and HF stimulation induced changes in network excitability.

Post-operative CT, and pre-operative T1-weighted MRI (MPRAGE) images were used for lead localization. Open source Lead DBS imaging package (v2.5.3) was used for thalamus electrode localization relative to the Krauth/Morel atlas¹³. Extra-thalamic lead localization and patient specific image rendering was performed using FreeSurfer 7 and custom scripts, along with the Destrieux atlas²⁴. Group electrode renderings in Montreal Neurological Institute (MNI) space were completed using SPM12 and custom scripts (Fig. 2). All statistical analyses were performed using MATLAB (v2020b, MathWorks).

This work was supported by: National Institute of Mental Health Award R01MH122258. The content is solely the responsibility of the authors and does not represent the official views of the NIH.

Conflicts of interest: N.M.G. is an industry consultant (NeuroOne, funds to Mayo Clinic). G.A.W. declares intellectual property has been licensed to Cadence Neuroscience and NeuroOne. G.A.W. serves on scientific advisory board for NeuroOne Inc., UNEEG Inc., LivaNova Inc., and NeuroPace Inc. B.N.L. declares intellectual property licensed to Cadence Neuroscience (contractual rights waived) and Seer Medical (contractual rights waived); and has been a site investigator (Medtronic EPAS, NeuroPace RESPONSE, Neuroelectrics tDCS for Epilepsy) and industry consultant (Epiminder, Medtronic, Neuropace, Philips Neuro; funds to Mayo Clinic). J.J.V.G. was named inventor for intellectual property licensed to Cadence Neuroscience, and has been an investigator for the Medtronic EPAS trial, SLATE trial, and Mayo Clinic Medtronic NIH Public Private Partnership (UH3-NS95495); has owned stock in and has had a consulting contract with Neuro-One; and has been site Primary Investigator in the Polyganics ENCASE II trial, site Primary Investigator in the NXDC Gleolan Men301 trial, and site Primary Investigator in the Insightec MRgUS EP001 trial. Remaining authors declare no competing financial interests.

Author Contributions: N.M.G., D.H., G.A.W. designed research; N.M.G., D.H., G.A.W., G.O.V, H.H., performed research; N.M.G., D.H., H.H., K.J.M. contributed analytic tools; N.M.G. and D.H. wrote the paper; all authors provided meaningful drafting and editing of the paper.

References

1. Benabid AL, Pollak P, Louveau A, Henry S, de Rougemont J. Combined (thalamotomy and stimulation) stereotactic surgery of the VIM thalamic nucleus for bilateral Parkinson disease. *Appl Neurophysiol.* 1987;50(1-6):344-346.
2. Schuepbach WM, Rau J, Knudsen K, et al. Neurostimulation for Parkinson's disease with early motor complications. *N Engl J Med.* 2013;368(7):610-622.
3. Fisher R, Salanova V, Witt T, et al. Electrical stimulation of the anterior nucleus of thalamus for treatment of refractory epilepsy. *Epilepsia.* 2010;51(5):899-908.
4. Ashkan K, Rogers P, Bergman H, Ughratdar I. Insights into the mechanisms of deep brain stimulation. *Nat Rev Neurol.* 2017;13(9):548-554.
5. Fisher RS, Acevedo C, Arzimanoglou A, et al. ILAE official report: a practical clinical definition of epilepsy. *Epilepsia.* 2014;55(4):475-482.
6. Piper RJ, Richardson RM, Worrell G, et al. Towards network-guided neuromodulation for epilepsy. *Brain.* 2022;145(10):3347-3362.
7. Karoly PJ, Rao VR, Gregg NM, et al. Cycles in epilepsy. *Nature Reviews Neurology.* 2021.
8. Keller CJ, Honey CJ, Megevand P, Entz L, Ulbert I, Mehta AD. Mapping human brain networks with cortico-cortical evoked potentials. *Philos Trans R Soc Lond B Biol Sci.* 2014;369(1653).
9. van Blooij D, van den Boom MA, van der Aar JF, et al. Developmental trajectory of transmission speed in the human brain. *Nat Neurosci.* 2023;26(4):537-541.
10. Keller CJ, Huang Y, Herrero JL, et al. Induction and Quantification of Excitability Changes in Human Cortical Networks. *J Neurosci.* 2018;38(23):5384-5398.
11. Valentin A, Alarcon G, Honavar M, et al. Single pulse electrical stimulation for identification of structural abnormalities and prediction of seizure outcome after epilepsy surgery: a prospective study. *Lancet Neurol.* 2005;4(11):718-726.
12. Matsumoto R, Kunieda T, Nair D. Single pulse electrical stimulation to probe functional and pathological connectivity in epilepsy. *Seizure.* 2017;44:27-36.
13. Krauth A, Blanc R, Poveda A, Jeanmonod D, Morel A, Szekely G. A mean three-dimensional atlas of the human thalamus: generation from multiple histological data. *Neuroimage.* 2010;49(3):2053-2062.
14. Horn A, Li N, Dembek TA, et al. Lead-DBS v2: Towards a comprehensive pipeline for deep brain stimulation imaging. *Neuroimage.* 2019;184:293-316.
15. Amunts K, Lepage C, Borgeat L, et al. BigBrain: an ultrahigh-resolution 3D human brain model. *Science.* 2013;340(6139):1472-1475.
16. Charlebois CM, Anderson DN, Johnson KA, et al. Patient-specific structural connectivity informs outcomes of responsive neurostimulation for temporal lobe epilepsy. *Epilepsia.* 2022;63(8):2037-2055.
17. Horn A, Reich M, Vorwerk J, et al. Connectivity Predicts deep brain stimulation outcome in Parkinson disease. *Ann Neurol.* 2017;82(1):67-78.
18. Johnson KA, Duffley G, Anderson DN, et al. Structural connectivity predicts clinical outcomes of deep brain stimulation for Tourette syndrome. *Brain.* 2020;143(8):2607-2623.
19. Middlebrooks EH, Okromelidze L, Wong JK, et al. Connectivity correlates to predict essential tremor deep brain stimulation outcome: Evidence for a common treatment pathway. *Neuroimage Clin.* 2021;32:102846.

20. Salanova V, Sperling MR, Gross RE, et al. The SANTE study at 10 years of follow-up: Effectiveness, safety, and sudden unexpected death in epilepsy. *Epilepsia*. 2021;62(6):1306-1317.
21. Turrigiano GG. The self-tuning neuron: synaptic scaling of excitatory synapses. *Cell*. 2008;135(3):422-435.
22. Stieve BJ, Richner TJ, Krook-Magnuson C, Netoff TI, Krook-Magnuson E. Optimization of closed-loop electrical stimulation enables robust cerebellar-directed seizure control. *Brain*. 2023;146(1):91-108.
23. Huang H, Gregg NM, Valencia GO, et al. Electrical stimulation of temporal and limbic circuitry produces distinct responses in human ventral temporal cortex. *J Neurosci*. 2023.
24. Destrieux C, Fischl B, Dale A, Halgren E. Automatic parcellation of human cortical gyri and sulci using standard anatomical nomenclature. *Neuroimage*. 2010;53(1):1-15.